Localization effects in quantum percolation

Gerald Schubert,[1] Alexander Weiße,[2] and Holger Fehske[1]
[1]*Institut für Physik, Ernst-Moritz-Arndt Universität Greifswald, D-17487 Greifswald, Germany*
[2]*School of Physics, The University of New South Wales, Sydney, New South Wales 2052, Australia*
(Received 30 June 2004; published 26 January 2005)

We present a detailed study of the quantum site percolation problem on simple cubic lattices, thereby focusing on the statistics of the local density of states and the spatial structure of the single particle wave functions. Using the kernel polynomial method we refine previous studies of the metal-insulator transition and demonstrate the nonmonotonic energy dependence of the quantum percolation threshold. Remarkably, the data indicates a "fragmentation" of the spectrum into extended and localized states. In addition, the observation of a chequerboardlike structure of the wave functions at the band center can be interpreted as anomalous localization.

DOI: 10.1103/PhysRevB.71.045126 PACS number(s): 71.23.An, 71.30.+h, 05.60.Gg, 72.15.Rn

Disordered structures attracted continuing interest over the last decades, and in addition to the Anderson localization problem[1] quantum percolation[2,3] is one of the classical subjects of this field. Current applications concern, e.g., transport properties of doped semiconductors[4] and granular metals,[5] metal-insulator transitions in two-dimensional *n*-GaAs heterostructures,[6] wave propagation through binary inhomogeneous media,[7] superconductor-insulator and (integer) quantum Hall transitions,[8,9] or the dynamics of atomic Fermi-Bose mixtures.[10] Another important example is the metal-insulator transition in perovskite manganite films and the related colossal magnetoresistance effect, which in the meantime are believed to be inherently percolative.[11]

In disordered solids the percolation problem is characterized by the interplay of pure classical and quantum effects. Apart from the question of finding a percolating path of "accessible" sites through a given lattice the quantum nature of the electrons imposes further restrictions on the existence of extended states and, consequently, of a finite dc conductivity. As a particularly simple model describing this situation we consider a tight-binding one-electron Hamiltonian

$$H = \sum_{i=1}^{N} \epsilon_i c_i^\dagger c_i - t \sum_{\langle ij \rangle} (c_i^\dagger c_j + \text{H.c.}) \tag{1}$$

on a simple cubic lattice with $N=L^3$ sites and random on-site energies ϵ_i drawn from the bimodal distribution

$$p(\epsilon_i) = p\,\delta(\epsilon_i - \epsilon_A) + (1-p)\,\delta(\epsilon_i - \epsilon_B). \tag{2}$$

The two energies ϵ_A and ϵ_B could, for instance, represent the potential landscape of a binary alloy A_pB_{1-p}, where each site is occupied by an *A* or *B* atom with probability p or $1-p$, respectively. In the limit $\Delta=(\epsilon_B-\epsilon_A)\to\infty$ the wave function of the *A* subband vanishes identically on the *B* sites, making them completely inaccessible for the quantum particles. We then arrive at a situation where noninteracting electrons move on a random ensemble of lattice points, which, depending on p, may span the entire lattice or not. The corresponding Hamiltonian reads

$$H = -t \sum_{\langle ij \rangle \in A} (c_i^\dagger c_j + \text{H.c.}), \tag{3}$$

where the summation extends over nearest-neighbor *A* sites only and, without loss of generality, ϵ_A is chosen to be zero.

Within the classical percolation scenario the percolation threshold p_c is defined by the occurrence of an infinite cluster A_∞ of adjacent *A* sites. For the simple cubic lattice this site-percolation threshold is $p_c=0.3117$.[12] In the quantum case, the multiple scattering of the particles at the irregular boundaries of the cluster can suppress the wave function, in particular, within narrow channels or close to dead ends of the cluster. Hence, this type of disorder can lead to absence of diffusion due to localization, even if there is a classical percolating path through the crystal. On the other hand, for finite Δ the tunneling between *A* and *B* sites may cause a finite dc conductivity although the *A* sites are not percolating. Naturally, the question arises whether the quantum percolation threshold p_q, given by the probability above which an extended wave function exists within the *A* subband, is larger or smaller than p_c. Previous results[13] for finite values of Δ indicate that the tunneling effect has a marginal influence on the percolation threshold as soon as $\Delta \gg 4tD$, where D denotes the spatial dimension of the hypercubic lattice.

In the theoretical investigation of disordered systems it turned out that distribution functions for the random quantities take the center stage.[1,14] The distribution $f[\rho_i(E)]$ of the local density of states (LDOS)

$$\rho_i(E) = \sum_{n=1}^{N} |\psi_n(\mathbf{r}_i)|^2 \delta(E - E_n) \tag{4}$$

is particularly suited because $\rho_i(E)$ measures the local amplitude of the wave function at site $\mathbf{r}_i$. It therefore contains direct information about the localization properties. In contrast to the (arithmetically averaged) mean DOS, $\rho_{\text{me}}(E) = \langle \rho_i(E) \rangle$, the LDOS becomes critical at the localization transition.[15,16] The probability density $f[\rho_i(E)]$ was found to have essentially different properties for extended and localized phases.[17] For an extended state at energy E the amplitude of the wave functions is more or less uniform. Accord-

ingly $f[\rho_i(E)]$ is sharply peaked and symmetric about $\rho_{\mathrm{me}}(E)$. On the other hand, if states become localized, the wave function has considerable weight only on a few sites. In this case the LDOS strongly fluctuates throughout the lattice and the corresponding LDOS distribution is very asymmetric and has a long tail. Above the localization transition the distribution of the LDOS is singular, i.e., mainly concentrated at $\rho_i=0$. Nevertheless the rare but large LDOS values dominate the mean DOS $\rho_{\mathrm{me}}(E)$, which therefore cannot be taken as a good approximation of the most probable value of the LDOS. Such systems are referred to as "non-self-averaging." Of course, for practical calculations the recording of entire distributions is a bit inconvenient. Instead the mean DOS $\rho_{\mathrm{me}}(E)$ together with the (geometrically averaged) so-called "typical" DOS, $\rho_{\mathrm{ty}}(E)=\exp\langle \ln \rho_i(E)\rangle$, is frequently used to monitor the transition from extended to localized states. The typical DOS puts sufficient weight on small values of ρ_i and a comparison to $\rho_{\mathrm{me}}(E)$ therefore allows one to detect the localization transition. This has been shown for the pure Anderson model[16,18,19] and for even more complex situations, where the effects of correlated disorder,[20] electron-electron interaction[21,22] or electron-phonon coupling[23,24] were taken into account.

In this paper we employ the typical-DOS concept to analyze the nature of the eigenstates (extended or localized) of the Hamiltonians (1) and (3). Using the kernel polynomial method,[18,25] an efficient high-resolution Chebyshev expansion technique, in a first step, we calculate the LDOS for a large number of samples K_r and sites K_s. The mean DOS is then simply given by

$$\rho_{\mathrm{me}}(E)=\frac{1}{K_rK_s}\sum_{k=1}^{K_r}\sum_{i=1}^{K_s}\rho_i(E), \tag{5}$$

whereas the typical DOS is obtained from the geometric average

$$\rho_{\mathrm{ty}}(E)=\exp\left(\frac{1}{K_rK_s}\sum_{k=1}^{K_r}\sum_{i=1}^{K_s}\ln[\rho_i(E)]\right). \tag{6}$$

We classify a state at energy E with $\rho_{\mathrm{me}}(E)\neq 0$ as localized if $\rho_{\mathrm{ty}}(E)=0$ and as extended if $\rho_{\mathrm{ty}}(E)\neq 0$.

Before discussing possible localization phenomena let us investigate the behavior of the mean DOS for the quantum percolation models (1) and (3). Figure 1 shows that as long as ϵ_A and ϵ_B do not differ too much there exists an asymmetric (if $p\neq 0.5$) but still connected electronic band.[13] At about $\Delta\simeq 4tD$ this band separates into two subbands centered at ϵ_A and ϵ_B, respectively. The most prominent feature in the split-band regime is the series of spikes at discrete energies within the band. As an obvious guess, we might attribute these spikes to eigenstates on islands of A or B sites being isolated from the main cluster.[2,26] It turns out, however, that some of the spikes persist, even if we neglect all finite clusters and restrict the calculation to the spanning cluster of A sites A_∞. This is illustrated in the upper panels of Fig. 2, where we compare the DOS of the models (1) [at $\Delta\to\infty$] and (3). Increasing the concentration of accessible sites the mean DOS of the spanning cluster is evocative of the DOS of the simple

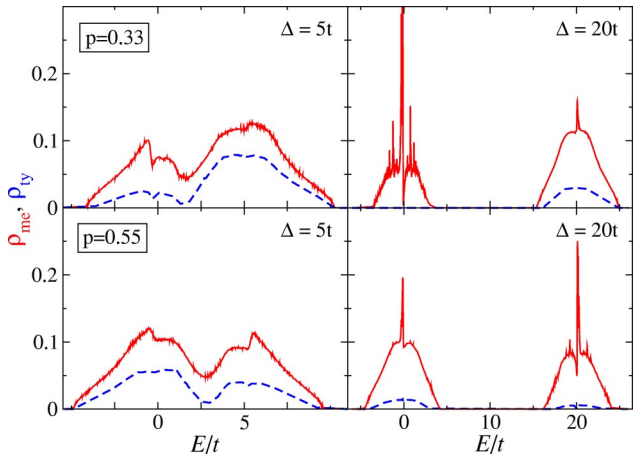

FIG. 1. (Color online) Mean (red solid line) and typical (blue dashed line) DOS of the Hamiltonian (1) on a 50^3 lattice with periodic boundary conditions (PBC). Results are obtained using $M=32\,768$ Chebyshev moments and $K_s\times K_r=32\times 32$ realizations.

cubic lattice, but even at large values of p a sharp peak structure remains at $E=0$ (see Fig. 2, lower panels).

To elucidate this effect, which partially is not accounted for in the literature,[2,13,27,28] in more detail, in Fig. 3 we fixed p at 0.33, shortly above the classical percolation threshold, and increased the ensemble size. In addition to the most dominant peaks at $E/t=0,\pm 1,\pm\sqrt{2}$. We can also resolve distinct spikes at $E/t=\frac{1}{2}(\pm 1\pm\sqrt{5}),\pm\sqrt{3},\pm\sqrt{2\pm\sqrt{2}}$, etc. These special energies coincide with the eigenvalues of the tight-binding model on small clusters of the geometries shown in the right part of Fig. 3. In accordance with Refs. 2 and 29 we can thus argue that the wave functions, which correspond to these special energies, are localized on some "dead ends" of the spanning cluster.

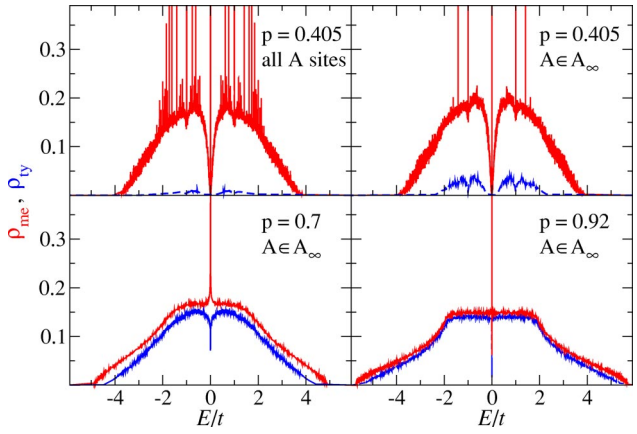

FIG. 2. (Color online) Mean (red solid line) and typical (blue dashed line) DOS for the quantum percolation model in the limit $\Delta\to\infty$. While in the upper left panel all A sites are taken into account, the other three panels show data for the restricted model (3) on the spanning cluster A_∞ only (note that ρ_{ty} is smaller in the former case because there are more sites with vanishing amplitude of the wave function). System sizes were adapted to ensure that A_∞ always contains the same number of sites, i.e., $N=57^3$ for $p=0.405$, 46^3 for $p=0.70$, and 42^3 for $p=0.92$. Again we used $M=32768$ and $K_s\times K_r=32\times 32$.

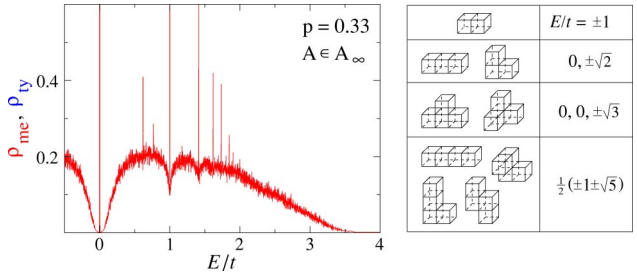

FIG. 3. (Color online) Left: Mean DOS for the model (3) with $p=0.33$ on a 100^3 lattice (PBC, $M=32\,768$). Data obtained from an average over 100 random initializations of sites for $K_r=100$ realizations of disorder. Note that $\rho_{ty}<10^{-5}$ holds in the whole band. Right: Some cluster configurations related to the special energies at which the peaks in ρ_{me} occur.

The assumption that the distinct peaks correspond to localized wave functions is corroborated by the fact that the typical DOS vanishes or, at least, shows a dip at these energies. Occurring also for finite Δ (Fig. 1), this effect becomes more pronounced as $\Delta\to\infty$ and in the vicinity of the classical percolation threshold p_c. From the study of the Anderson model[1] we know that localization leads at first to a narrowing of the energy window containing extended states. The corresponding mobility edges have been mapped out with high precision.[19,30] For the percolation problem, in contrast, with decreasing p the typical DOS indicates both localization from the band edges and localization at particular energies within the band. Since finite cluster wave functions such as those shown in Fig. 3 can be constructed for numerous other, less probable geometries,[31] Chayes *et al.*[29] argued that an infinite discrete series of such spikes might exist within the spectrum. The picture of localization in the quantum percolation model is then quite remarkable. If we generalize our numerical data for the peaks at $E=0$ and $E/t=\pm1$, it seems as if there is an infinite discrete set of energies with localized wave functions, which is dense within the entire spectrum. In between there are continua of delocalized states, but to avoid mixing, their density goes to zero close to the localized states. Facilitated by the large special weight of the peak (up to 10% close to p_c) this is clearly observed at $E=0$, and we suspect similar behavior at $E/t=\pm1$. For the other discrete spikes the resolution of our numerical data is still too poor and the system size might be even too small to draw a definite conclusion.

In order to understand the internal structure of the extended and localized states we calculated the amplitudes of the wave function at specific energies for a random sample of the quantum percolation model (3) restricted to A_∞. Figure 4 visualizes the spatial variation of $|\psi_n(\mathbf{r}_i)|$ on a 14^3 lattice with PBC and an occupation probability $p=0.45$ well above the classical percolation threshold. The figure clearly indicates that the state with $E/t=0.66$ is extended, i.e., the spanning cluster is quantum mechanically "transparent." On the contrary, at $E=t$, the wave function is completely localized on a finite region of the spanning cluster. Here the scattering of the particle at the random surface of the spanning cluster results in states, where the wave function vanishes identically except for some finite domains on loose ends (similar

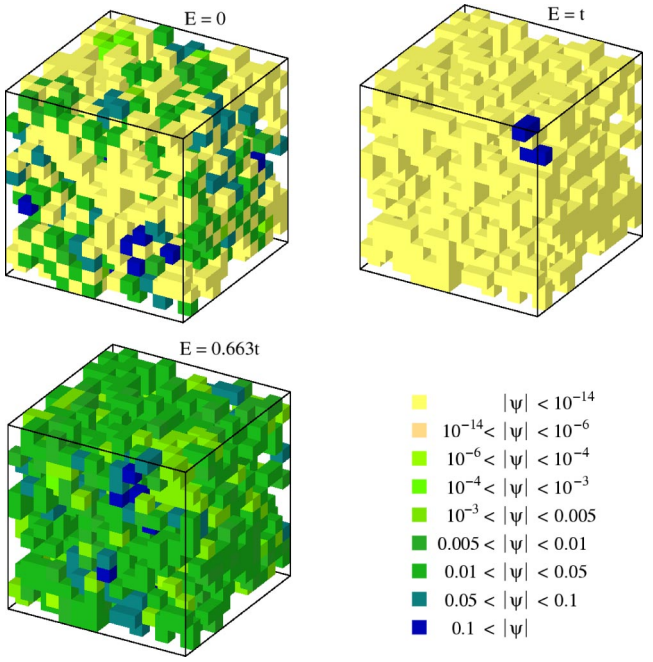

FIG. 4. (Color online) Amplitudes of the wave function $|\psi_n(\mathbf{r}_i)|$ of the quantum percolation model (3) on A_∞ of a 14^3 lattice with occupation probability $p=0.45$. Exact diagonalization results are presented at three characteristic energies $E/t=0$, 1, and 0.663 corresponding to anomalously localized, localized, and delocalized states, respectively.

to those shown in Fig. 3), where it takes the values $(\pm1,\mp1)$, $(\pm1,\mp1,0,\mp1,\pm1),\ldots$. Note that these regions are part of the spanning cluster, connected to the other sites by a site with wave function amplitude zero. A particularly interesting behavior is observed at $E=0$. The eigenstate $E=0$ is highly degenerate and we can form wave functions that span the entire lattice in a chequerboard structure with zero and nonzero amplitudes (see Fig. 4). Although these states are extended in the sense that they are not confined to some region of the cluster, they are localized in the sense that they do not contribute to the dc conductivity. This is caused by the alternating structure which suppresses the nearest-neighbor hopping, and in spite of the high degeneracy, the current matrix element between different $E=0$ states is zero. Hence, having properties of both classes of states these states are called anomalously localized.[4,32] The chequerboard structure is also observed for the hypercubic lattice in 2D but with reduced spectral weight, compared to the 3D case. Another indication for the robustness of this feature is its persistence for mismatching boundary conditions, e.g., periodic (antiperiodic) boundary conditions for odd (even) values of the linear extension L. In these cases the chequerboard is matched to itself by a manifold of sites with vanishing amplitude.

In the past most of the methods used in numerical studies of Anderson localization have also been applied to the percolation models (1) and (3) in order to determine the quantum percolation threshold p_q, defined as the probability p below which all states are localized (see, e.g., Refs. 3,33, and references therein). However, so far the results for p_q are

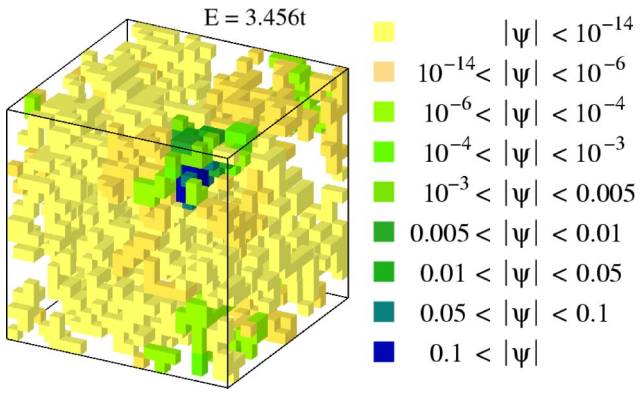

FIG. 5. (Color online) Amplitudes $|\psi_n(\mathbf{r}_i)|$ of a localized state on a 21^3 lattice with $p=0.33$ obtained by exact diagonalization of the model (3). $E/t=3.456$ was chosen in order to avoid any of the special cluster configurations discussed above.

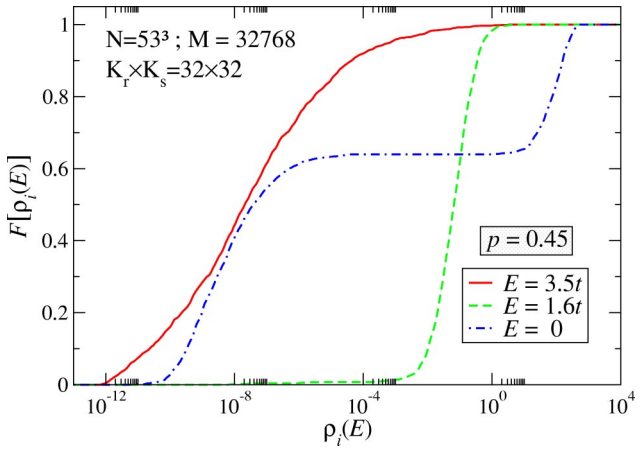

FIG. 7. (Color online) Characteristic probability distributions of the LDOS.

far less precise than, e.g., the values of the critical disorder reported for the Anderson model. For the simple cubic lattice numerical estimates of quantum site-percolation threshold range from 0.4 to 0.5. In Figs. 1–3 we presented data for ρ_{ty} which indicates that $p_q > p_c$. In fact, within numerical accuracy, we found $\rho_{\mathrm{ty}}=0$ for $p=0.33>p_c$. Figure 5 displays the amplitude of a typical state obtained by exact diagonalization for a fixed realization of disorder. Bearing in mind that we have used PBC, the support of the wave function appears to be a finite (connected) region of the spanning cluster A_∞, i.e., the state is clearly localized.

To get a more detailed picture we calculated the normalized typical DOS, $R(p,E)=\rho_{\mathrm{ty}}/\rho_{\mathrm{me}}$, in the whole concentration-energy plane. Figure 6 presents such kind of phase diagram of the quantum percolation model (3). The data supports a finite quantum percolation threshold $p_q \gtrsim 0.4 > p_c$ (See also Refs. 13 and 33–35), but as the discussion above indicated, for $E=0$ and $E=\pm t$ the critical

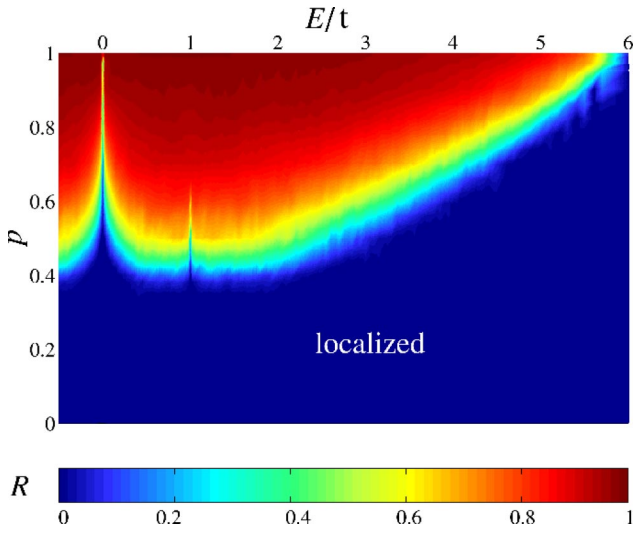

FIG. 6. (Color online) Normalized typical DOS $R=\rho_{\mathrm{ty}}/\rho_{\mathrm{me}}$ in the concentration-energy plane for the model (3) on a 50^3 lattice for $p \geqslant 0.5$ and a 100^3 lattice for $p<0.5$. We used $M=16\,384$ Chebyshev moments and averaged over $K_s \times K_r = 32 \times 32$ realizations.

value $p_q(E)$ is 1, and the same may hold for the set of other "special" energies. The transition line between localized and delocalized states, $p_q(E)$, might thus be a rather irregular (fractal?) function. On the basis of our numerical treatment, however, we are not in the position to answer this question with full rigour.

Finally let us come back to the characterization of extended and localized states in terms of distribution functions. Figure 7 displays the probability distribution

$$F[\rho_i(E)] = \int_0^{\rho_i(E)} f[\rho_i'(E)]d\rho_i'(E), \tag{7}$$

for three typical energies $E/t=3.5$, 1.6, and 0 corresponding to localized, extended, and anomalously localized states at $p=0.45$, respectively. The differences in $F[\rho_i(E)]$ are significant. The slow increase of $F[\rho_i(E)]$ observed for localized states corresponds to an extremely broad LDOS distribution, with a very small most probable (or typical) value of $\rho_i(E)$. This is in agreement with the findings for the Anderson model.[18,19] Accordingly the jumplike increase found for extended states is related to an extremely narrow distribution of the LDOS centered around the mean DOS, where ρ_{me} coincides with the most probable value. At $E=0$, the probability distribution exhibits two steps, leading to a bimodal distribution density. Here the first (second) maximum is related to sites with a small (large) amplitude of the wave function—a feature that substantiates the chequerboard structure discussed above.

To summarize, we have demonstrated the value and power of the probability distribution approach to quantum percolation. As for standard Anderson localization the typical density of states can serve as a kind of order parameter differentiating between extended and localized states. Our numerical data corroborates previous results in favor of a quantum percolation threshold $p_q > p_c$ and a fragmentation of the spectrum into extended and localized states. The latter refers to a discrete but dense set of localized states separated by continua of delocalized states. Accordingly the function $p_q(E)$ is rather irregular. At the band center, so-called anoma-

lous localization is observed, which manifests itself in a chequerboardlike structure of the wave function. Even though the kernel polynomial method allows for the study of very large clusters with high-energy resolution, the quantum percolation problem certainly deserves further investigation.

It is a pleasure to acknowledge useful discussions with A. Alvermann, F.X. Bronold, G. Wellein, and W. Weller. Special thanks go to LRZ München, NIC Jülich, and HLRN (Zuse-Institut Berlin) for granting resources on their supercomputing facilities.

[1] P. W. Anderson, Phys. Rev. **109**, 1492 (1958).
[2] S. Kirkpatrick and T. P. Eggarter, Phys. Rev. B **6**, 3598 (1972).
[3] A. Mookerjee, I. Dasgupta, and T. Saha, Int. J. Mod. Phys. B **9**, 2989 (1995).
[4] M. Inui, S. A. Trugman, and E. Abrahans, Phys. Rev. B **49**, 3190 (1994).
[5] M. V. Feigel'man, A. Ioselevich, and M. Skvortsov, Phys. Rev. Lett. **93**, 136403 (2004).
[6] S. Das Sarma, M. P. Lilly, E. H. Hwang, L. N. Pfeiffer, K. W. West, and J. L. Reno, cond-mat/0406655 (unpublished).
[7] Y. Avishai and J. Luch, Phys. Rev. B **45**, 1074 (1992).
[8] Y. Dubi, Y. Meir, and Y. Avishai, cond-mat/0406008 (unpublished).
[9] N. Sandler, H. Maei, and J. Kondev, Phys. Rev. B **70**, 045309 (2004).
[10] A. Sanpera *et al.*, Phys. Rev. Lett. **93**, 040401 (2004).
[11] T. Becker, C. Streng, Y. Luo, V. Moshnyaga, B. Damaschke, N. Shannon, and K. Samwer, Phys. Rev. Lett. **89**, 237203 (2002).
[12] D. W. Heermann and D. Stauffer, Z. Phys. B: Condens. Matter **44**, 339 (1981).
[13] C. M. Soukoulis, Q. Li, and G. S. Grest, Phys. Rev. B **45**, 7724 (1992).
[14] R. Abou-Chacra, P. W. Anderson, and D. J. Thouless, J. Phys. C **6**, 1734 (1973).
[15] R. Haydock and R. L. Te, Phys. Rev. B **49**, 10 845 (1994).
[16] V. Dobrosavljević, A. A. Pastor, and B. K. Nikolić, Europhys. Lett. **62**, 76 (2003).
[17] A. D. Mirlin and Y. V. Fyodorov, J. Phys. I **4**, 655 (1994).
[18] G. Schubert, A. Weiße, G. Wellein, and H. Fehske, *High Performance Computing in Science and Engineering*, edited by S. Wagner, W. Hanke, A. Bode, and F. Durst (Springer, Berlin, 2005).
[19] A. Alvermann, G. Schubert, A. Weiße, F. X. Bronold, and H. Fehske, cond-mat/0406051 (unpublished).
[20] G. Schubert, A. Weiße, and H. Fehske, cond-mat/0406212 (unpublished).
[21] V. Dobrosavljević and G. Kotliar, Phys. Rev. Lett. **78**, 3943 (1997).
[22] K. Byczuk, W. Hofstetter, and D. Vollhardt, cond-mat/0403765 (unpublished).
[23] F. X. Bronold and H. Fehske, Phys. Rev. B **66**, 073102 (2002).
[24] F. X. Bronold, A. Alvermann, and H. Fehske, Phys. Status Solidi C **1**, B63 (2004).
[25] R. N. Silver, H. Röder, A. F. Voter, and D. J. Kress, J. Comput. Phys. **124**, 115 (1996).
[26] R. Berkovits and Y. Avishai, Phys. Rev. B **53**, R16 125 (1996).
[27] T. Odagaki, N. Ogita, and H. Matsuda, J. Phys. C **13**, 189 (1980).
[28] C. M. Soukoulis, E. N. Economou, and G. S. Grest, Phys. Rev. B **36**, 8649 (1987).
[29] J. T. Chayes, L. Chayes, J. R. Franz, J. P. Sethna, and S. A. Trugman, J. Phys. A **19**, L1173 (1986).
[30] A. Mac Kinnon and B. Kramer, Z. Phys. B: Condens. Matter **53**, 1 (1983).
[31] G. Schubert, Diploma thesis, Universität Bayreuth, 2003.
[32] Y. Shapir, A. Aharony, and A. B. Harris, Phys. Rev. Lett. **49**, 486 (1982).
[33] T. Koslowski and W. von Niessen, Phys. Rev. B **42**, 10 342 (1990).
[34] A. Kusy, A. W. Stadler, G. Hałdaś, and R. Sikora, Physica A **241**, 403 (1997).
[35] A. Kaneko and T. Ohtsuki, J. Phys. Soc. Jpn. **68**, 1488 (1999).